

O. P. Posnansky<sup>1</sup>, and N. J. Shah<sup>1,2</sup>

<sup>1</sup>Institute of Neuroscience and Biophysics 3 - Medicine, Research Centre Juelich, Juelich, Germany, <sup>2</sup>Faculty of Medicine, Department of Neurology, RWTH Aachen University, JARA, Aachen, Germany

**1. Introduction:** Water diffusion in neurological tissues is known to exhibit multi-component diffusion behaviour. The random motion of water molecules is in accordance with the structure peculiarities and the physical properties of composite brain white matter. We simulate the complex behaviour of water molecules using the *Basser-Sen* model [1] and the renormalization group (RG) method [2,3] (in this study we do not use the Maxwell-Garnett approximation adapted in [2,3]). In the context of the modelling framework, we explore a bridge between local and effective global diffusive transport properties and estimate the sensitivity of the diffusion coefficient to the dominant set of micro-parameters: extracellular volume fraction, extracellular diffusion, myelin-sheath diffusion, axon diffusion, mean size of axon, mean size of myelin-sheath, extra-cellular proton density, myelin-sheath proton density, and axon proton density.

**2. Methods:** Brain white matter has a very complex, multi compartmental structure. In general it comprises myelinated axons immersed in extracellular matrix. Axons are distributed chaotically and, for convenience, they can be treated as ideal cylinders. Following the *Basser-Sen* model, we characterize coated fibres by  $D_m$  (myelin-sheath diffusion),  $D_a$  (axon diffusion) and corresponding proton densities  $c_a, c_m$ , which have outer ( $R_m$ ) and inner ( $R_a$ ) radius. Such a fibre is immersed in an extra-cellular space, the Wigner-Seitz (WS) cell, with diffusion  $D_t$ , proton density  $c_t$  and linear size  $L$  (Fig.1). It is possible to calculate the diffusive properties of WS cell using the *Basser-Sen* model for the case when WS is occupied with a fibre and the empty WS cell is assigned with extra-cellular properties. Two types of WS cells can be randomly distributed on the square lattice with probability  $p$  that WS cell is empty and  $(1-p)$  that WS is occupied with fibre (Fig.2, a black WS cell indicates fibre occupation). Such an approach is the opposite of the ordered spatial distribution of fibres described in the *Basser-Sen* model. On the square lattice with randomly occupied cells it is possible to outline 2x2 WS cell. All non-degenerative configurations of black and white WS cells on the scale 2x2 are presented in Fig.3. In Fig.4 the process of scale renormalization is depicted for the specific distribution of WS cells. Mathematically, such an RG process can be described by a system of nonlinear equations (Eq.1). In the Table1, equations for probability  $r_n^k$  and their degeneracy numbers for six classes of 2x2 cells (Fig.3) are presented. These equations comprise Eq.1a representing the RG process for an extra-cellular region. Eqs.(1c,d) were derived according to the rules given in the last column of Table1 and probability density (Eq.1b).

$$P_{n+1} = \sum_k g_k r_n^k \quad (1a)$$

$$P_{n+1} = (1-p_n) \delta(D_t - D_t^{L,n}) + p_n \delta(D_t - D_t^{U,n}) \quad (1b)$$

$$D_t^{U,n+1} = \langle D_t^{U,n} \rangle \quad (1c)$$

$$D_t^{L,n+1} = \langle D_t^{L,n} \rangle \quad (1d)$$

$$ADC_{eff} = (2D_t^{n \rightarrow \infty} + D_t)/3 \quad (2)$$

$$S = |\partial \log(ADC_{eff}) / \partial \log(X)| \quad (3)$$

Table 1

Class	Probability, $r_n^k$	Degeneracy, $g_k$	Effective diffusivity, $D_t^{U/L,n+1}$
I	$(1-p_n)^4$	1	$D_t^{L,n}$
II	$p_n^1 (1-p_n)^3$	4	$(2D_t^{L,n} D_t^{U,n} + D_t^{L,n} (D_t^{L,n} + D_t^{U,n})) / 2(D_t^{L,n} + D_t^{U,n})$
III	$p_n^2 (1-p_n)^4$	4	$(2D_t^{L,n} D_t^{U,n}) / (D_t^{L,n} + D_t^{U,n})$
IV	$p_n^2 (1-p_n)^4$	2	$(D_t^{L,n} + D_t^{U,n}) / 2$
V	$p_n^3 (1-p_n)^4$	4	$(2D_t^{L,n} D_t^{U,n} + D_t^{U,n} (D_t^{L,n} + D_t^{U,n})) / 2(D_t^{L,n} + D_t^{U,n})$
VI	$p_n^4$	1	$D_t^{U,n}$

Table 2

Parameter X	Input value
$D_t$	$2 \times 10^{-9} \text{ m}^2/\text{s}$
$D_a$	$.75 \times 10^{-9} \text{ m}^2/\text{s}$
$D_m$	$.3 \times 10^{-9} \text{ m}^2/\text{s}$
$c_t$	.95
$c_a$	.88
$c_m$	.5
$R_m$	$6.57 \times 10^{-6} \text{ m}$
$R_a$	$4 \times 10^{-6} \text{ m}$
$p$	[0, 1]

**3. Results:** We input the microscopic parameters,  $x$ , taken from Table2 into the *Basser-Sen* model to estimate lower ( $L$  superscript in notation, black square in Fig.2) and upper ( $U$  superscript in notation, white square in Fig.2) bounds of transverse diffusivity ( $t$  subscript in notation). Then we were solving Eq.1 for different values of  $p$ . During the RG process, effective diffusion approaches the stable point  $D_{t,n \rightarrow \infty} = D_t^{L,n \rightarrow \infty} = D_t^{U,n \rightarrow \infty}$  which depends on the extra-cellular volume fraction  $p$  (Fig.5). The number of  $n$ -steps in the RG trajectory is a function of  $p$  (Fig.6, changes of the effective diffusion are colour coded). In Fig.7 the dependence of longitudinal,  $D_t$ , transverse effective diffusion,  $D_{t,eff}$ , as well as  $ADC_{eff}$  (Eq.2) are presented. For comparison, we present the *classical Basser-Sen* results. We estimated the absolute value of the sensitivity,  $S$ , of  $ADC_{eff}$  to the various  $x$  micro-parameters changes (Eq.3) and plot pie chart with corresponding weights (Fig.8).

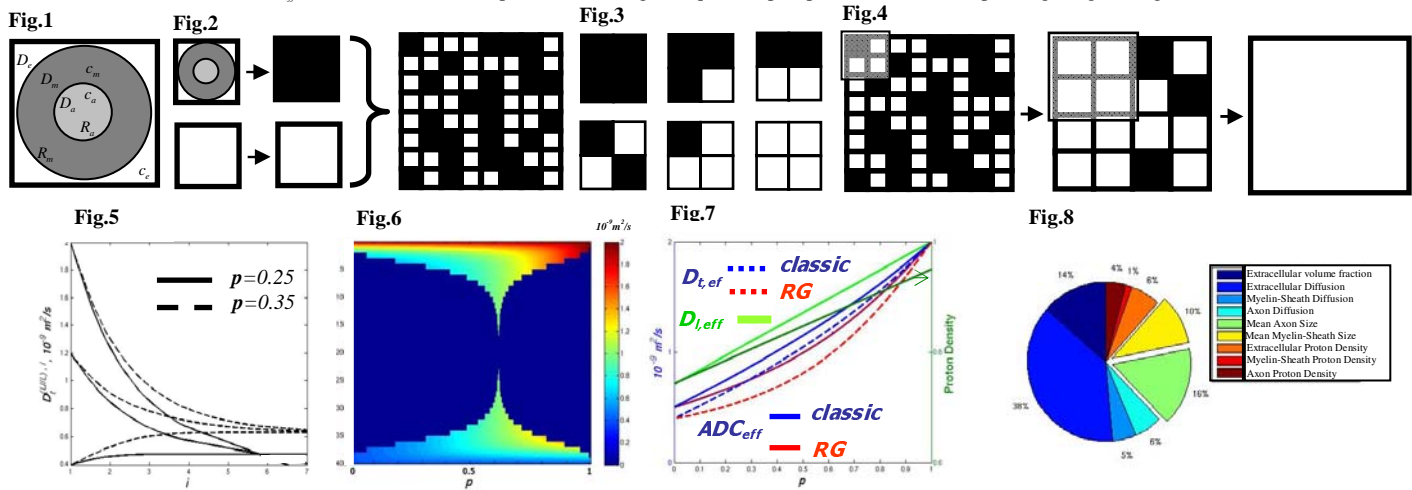


**Fig.1.** WS square cell occupied by myelinated fibre. The geometrical and physical parameters are labelled. **Fig.2.** Occupied and unoccupied WS cells imply upper (white) and lower (black) bounds of diffusivity. The WS cells are randomly distributed. **Fig.3.** Six basic configurations of WS cells with the scale 2x2. **Fig.4.** The RG procedure for cell 2x2. **Fig.5.** Approach of stable effective diffusivity after  $i$  RG-steps. **Fig.6.** Dependence of the number RG steps versus extra-cellular volume fraction. Evolution of diffusivity during the RG-process is colour-coded. **Fig.7.** Dependence of  $ADC_{eff}$ ,  $D_{t,eff}$ ,  $D_{t,eff}$  versus  $p$ . Every point in these curves is a result of the RG process. For comparison, the *Basser-Sen* results are shown. **Fig.8.** Pie chart of absolute values of the sensitivity,  $S$ , of  $ADC_{eff}$  near the physiologically relevant point ( $p \sim 0.2$ ).

**4. Discussion:** Using the RG method we have calculated the sensitivity of the  $ADC_{eff}$  to the different microparameters variations. We found that the  $ADC_{eff}$  exhibits its the strongest sensitivity to the extra-cellular volume fraction and diffusivity. These findings suggest a possible mechanism to explain  $ADC_{eff}$  changes during neurodegenerative disease progression. The  $ADC_{eff}$  demonstrates more nonlinear behaviour vs  $p$  changes due to blocking effects which are absent in ordered model of the brain white matter.

**References:** [1] Sen P, Basser P, *Biophys. J.*, **89** (2005) 2927. [2] Posnansky O., Shah N.J., *ISMRM2008*. [3] Posnansky O., Shah N.J., *J. Biol. Phys.*, *in press*.